Digital Communications and Networks 2 (2016) 57–64

HOSTED BY

Contents lists available at ScienceDirect

Digital Communications and Networks

journal homepage: www.elsevier.com/locate/dcan

Mitigating adjacent channel interference in vehicular communication systems

João Almeida [a,b,*], Muhammad Alam [a], Joaquim Ferreira [a,c], Arnaldo S.R. Oliveira [a,b]

[a] Instituto de Telecomunicações, Campus Universitário de Santiago, 3810-193 Aveiro, Portugal
[b] DETI - Universidade de Aveiro, Campus Universitário de Santiago, 3810-193 Aveiro, Portugal
[c] ESTGA - Universidade de Aveiro, 3754-909 Águeda, Portugal

ARTICLE INFO

Article history:
Received 10 February 2016
Accepted 10 March 2016
Available online 29 March 2016

Keywords:
Intelligent transportation systems
Vehicular communications
Adjacent Channel Interference
Filter design
Multi-rate systems
Digital Hardware Design

ABSTRACT

In the last few decades, dedicated wireless channels were specifically allocated to enable the development and implementation of vehicular communication systems. The two main protocol stacks, the WAVE standards proposed by the IEEE in the United States and the ETSI ITS-G5 in Europe, reserved 10 MHz wide channels in the 5.9 GHz spectrum band. Despite the exclusive use of these frequencies for vehicular communication purposes, there are still cross channel interference problems that have been widely reported in the literature. In order to mitigate these issues, this paper presents the design of a two-stage FIR low-pass filter, targeting the integration with a digital baseband receiver chain of a custom vehicular communications platform. The filter was tested, evaluated and optimized, with the simulation results proving the effectiveness of the proposed method and the low delay introduced in the overall operation of the receiver chain.

1. Introduction

Vehicular communications play a key role in the development of Intelligent Transportation Systems (ITS), whose main goal is the improvement of road safety and traffic efficiency. By extending the driver's field of view, vehicular networks can increase the time available to make decisions or to react in the case of traffic hazards. This way for instance, collisions in low visibility intersections and chain reaction crashes can be drastically reduced. In addition to this, value-added infotainment services can also be provided by vehicular communication systems, such as broadband internet connection or prices and locations of parking slots or gas stations.

There are two main protocol stacks for vehicular communications systems [1], enabling exchange of data among vehicles (V2V communications) and between vehicles and the road-side infrastructure (V2I/I2V). These two families of standards correspond to the IEEE Wireless Access in Vehicular Environments (WAVE), adopted in the United States, and the ETSI ITS-G5 in Europe. At the physical and medium access control layers, both protocol stacks rely on the IEEE 802.11p standard, an amendment to the IEEE 802.11 Wi-Fi reference [2]. In comparison with the typical Wi-Fi operation, there are just a number of modifications that are introduced to enhance the behavior of the communicating nodes under such dynamic scenarios. For instance, the channel bandwidth is reduced from 20 MHz to 10 MHz, in order to mitigate the effects of multi-path propagation and Doppler shift. As a consequence, the data rate is half of what can be obtained with standard Wi-Fi, i.e., from 3 Mbit/s to 27 Mbit/s instead of 6–54 Mbit/s. Another example is the introduction of non-IP messages that are broadcast outside the context of a Basic Service Set (BSS), avoiding the overhead introduced by the registration and authentication procedures, commonly present in wireless local area networks.

In order to guarantee that vehicular communications do not suffer from any type of interference from unlicensed devices, the Federal Communications Commission (FCC) in the United States and the European Conference of Postal and Telecommunications Administrations (CEPT) in Europe, allocated a dedicated spectrum band at 5.9 GHz (Fig. 1). In America, a bandwidth of 75 MHz was reserved, while in Europe only 50 MHz were assigned. This spectrum was divided into smaller 10 MHz wide channels and in the American case, a 5 MHz guard band at the low end was also included. As a result, there are 7 different channels for IEEE WAVE operation and 5 for the case of ETSI ITS-G5. In Europe, 30 MHz (3 channels) are reserved for road safety in the ITS-G5A band and 20 MHz are assigned for general purpose ITS services in the

* Corresponding author at: Instituto de Telecomunicações, Campus Universitário de Santiago, 3810-193 Aveiro, Portugal.
E-mail addresses: jmpa@ua.pt (J. Almeida), alam@av.it.pt (M. Alam), jjcf@ua.pt (J. Ferreira), arnaldo.oliveira@ua.pt (A.S.R. Oliveira).
Peer review under responsibility of Chongqing University of Posts and Telecommunications.

http://dx.doi.org/10.1016/j.dcan.2016.03.001

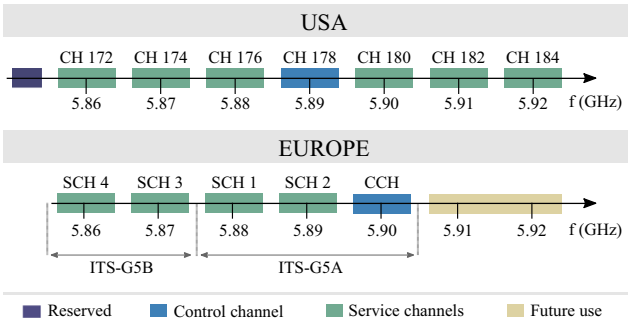

Fig. 1. Spectrum allocation for vehicular communications (adapted from [1]).

ITS-G5B band. As a general rule, a control channel (CCH 178 in the USA and CCH 180 in Europe) is exclusively used for cooperative road safety and control information. The remaining channels are designated as Service Channels (SCH). In the United States, concerns about the reduced capacity for road safety messages led to the decision to allocate SCH 172 specifically for applications regarding public safety of life and property [3]. Moreover, it is mandatory in Europe to have two radios in each vehicular communication platform, in order to guarantee at least one radio always tuned in the dedicated safety channel [4].

Notwithstanding the decision to allocate specific wireless channels for vehicular communication purposes, there are still issues with the operation of these systems, caused by the cross channel interference in the IEEE-WAVE/ETSI-ITS-G5 band and with the European tolling systems operating in the 5.8 GHz frequency band. The interference risks in the latter case were early identified by CEPT in 2007 [5] and several studies [6–8], simulation and experimental tests [9] were then conducted in order to evaluate the impact of ITS-G5 communications in a coexistence scenario with Electronic Toll Collection (ETC) systems. In these tests [9] organized by ETSI, the results have shown that under certain conditions, the ITS-G5 signals can harmfully interfere with ETC systems, causing a loss or non-completion of ETC transactions and/or a disruption of the stand-by mode of ETC On-Board Units (OBUs), i.e. the devices placed inside the vehicles.

Based on these findings, it was clear that the simultaneous operation of both systems at toll plazas could be seriously disturbed. This could lead to safety and congestion problems in these areas and cause substantial loss of revenues for road operators. It was also concluded that this interference is inevitable, unless ITS-G5 will adapt the transmitted power within a certain range around the tolling station or reduce the duty cycle of the message transmission. As a result, ETSI has introduced mandatory requirements for ITS-G5 stations to switch to a “protected mode” [7]. This shall be done when receiving information from any other ITS station containing the location of a tolling station. The ITS station that sends out the information about the tolling station location may either be a fixed located transmitter – Road-Side Unit (RSU) – in the vicinity of the tolling station, or it may also be an OBU in any vehicle that, in addition, is equipped with a 5.8 GHz toll detector.

Furthermore, there is also a perspective to use IEEE 802.11p for ETC communications, but studies [10] have shown it is possible that 802.11a based on-board devices operating in the 5 GHz band could degrade the performance of ETC systems based on vehicular communications. Simulation and real-world experiments [10] demonstrated an increase in the Packet Error Rate (PER) of the ETC 802.11p based system, when both technologies were working simultaneously. It was also shown that this effect cannot be removed by simply increasing the power transmitted by the 802.11p ETC units. In general, one can conclude that wireless communication systems operating near the 5.9 GHz frequency band pose serious problems to the performance of vehicular networks.

Nevertheless, the major source of interference in vehicular communications systems is the cross channel interference, generated by nodes communicating in the adjacent channels [11]. This Adjacent Channel Interference (ACI) can severely compromise the integrity of the messages received by a radio unit, whenever simultaneous communications occur in the nearby channels. Therefore, in order to reduce the effect of ACI in vehicular communication radio links, this paper presents the design of a two-stage Finite Impulse Response (FIR) filter, which guarantees an efficient suppression of the unwanted components of the received signal. At the same time, it is also ensured that few digital hardware resources are utilized and only a small delay is introduced in the receiver chain of the ITS-G5 station. The rest of the paper is organized as follows. Section 2 presents some related work and background on the topic of ACI in vehicular networks. Section 3 shows the effects of cross channel interference in the received signal of a custom vehicular communication platform, while Section 4 describes the design of the proposed digital filter and presents the obtained simulation results. Finally, Section 5 summarizes the concluding remarks and discusses some future work.

2. Related work and background

The IEEE WAVE and ETSI ITS-G5 protocol stacks establish a multi-channel architecture for vehicular communications, where different vehicles in the same geographical area can simultaneously transmit over the multiple channels presented in Fig. 1. This design decision produces obvious throughput improvements, however, since the parallel usage of adjacent channels can occur when vehicles are in the radio range of each other, interference between different nodes' transmissions may arise. This adjacent channel interference (ACI) can cause two main negative effects in the network communications [11]: an increased PER and a reduced transmission opportunity. In the former case, the Signal-to-Interference-plus-Noise-Ratio (SINR) of a packet being received by a node can be increased by another unit communicating in an adjacent channel, which may lead to the impossibility of correctly processing and decoding the frame. This will cause the loss of the packet and, if the situation is not momentary, it can result in large values of PER. The second mentioned effect occurs when a node wants to transmit a frame, but it perceives the channel as occupied due to a packet transmission in an adjacent channel. This channel busy indication is given by the Clear Channel Assessment (CCA) mechanism, being triggered by the power level sensed in the wireless medium, raised by the interferer in the nearby channel. In this situation, the potential transmitter will follow the back-off procedure specified by the CSMA method of IEEE 802.11 standard and thus the access to the wireless medium and the transmission of the intended message will be deferred. Moreover, it can happen that the packet decoding process in the potential receivers is not affected by the interferer, but the transmitter is still wrongly prevented to send its message. The ACI problem could be amplified in dual-radio units, as the ones in Europe, with antennas simultaneously operating on nearby channels and located in the same place, either in the same vehicle or road-side site.

In order to limit cross channel interference, the standard [2] specifies a spectrum emission mask that defines the out-of-band energy allowed for a transmitting device. This spectral mask is defined up to 15 MHz far from the center frequency and it becomes more stringent and difficult to comply with higher transmission power classes (A–D) [12]. On the receiver side, the standardization rules also establish a minimum Adjacent Channel Rejection (ACR) ratio for each modulation, measured by the power difference between the interfering signal and the signal in the desired channel. These masks are sufficient to avoid the most

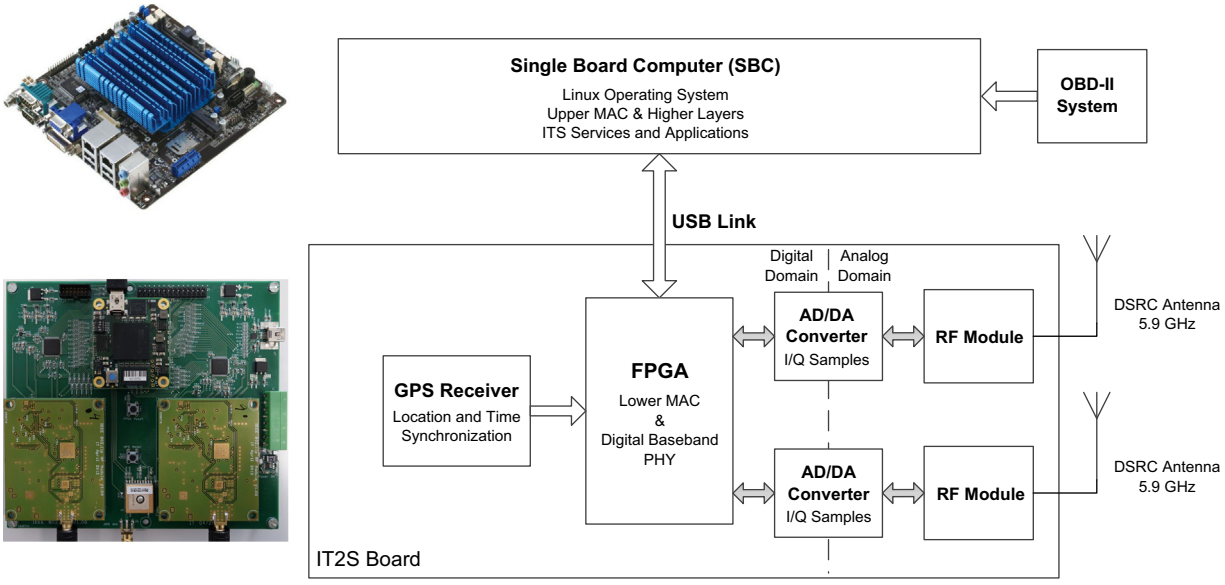

Fig. 2. IT2S platform architecture.

harmful interferences, particularly in the cases related to the blocking transmission effect. Nevertheless the impact on the PER can still be very severe under certain circumstances. Some preliminary field test results proved the large number of packet errors when an interferer working in an adjacent channel is close to the receiver node [13]. The distance for which the ACI effect starts to be critical (a PER higher than 10%) was measured and occurs whenever the interferer is closer than the intended transmitter to the receiver by an order of magnitude or more. Similar results were obtained in experimental simulations [14,15] and other field trial tests [16,17], confirming that the effect of cross channel interference cannot be neglected, specially under heavy traffic load conditions.

This issue is partially addressed in [18] by a token ring MAC protocol named MCTRP, aiming to improve throughput over all WAVE channels. The adaptive algorithm establishes virtual rings where groups of vehicles are organized, each one communicating in a specific service channel. By switching to a different SCH when the interference level increases, the protocol is able to reduce the ACI of a virtual ring. In [14], a preliminary solution to mitigate cross channel interference is proposed (Cross Channel CSMA/CA or 3CSMA/CA protocol), by reducing transmission power on the adjacent channel and by delaying potential transmissions until the reception on the adjacent channel is completed. The last measure is only taken depending if a potential receiver node is within a defined distance range or not. In order to protect safety messages exchanged on the control channel, Campolo and Molinaro [19] suggest the use of adjacent channels solely for vehicles temporarily stopped at sufficient distance from the road, such as in a gas station for refuelling. This way, it is possible to prevent a performance degradation in the CCH and at the same time, not completely waste the spectrum resources in the adjacent channels. To further reduce the effects of cross channel interference, disjoint contention window durations and Arbitrary Inter-Frame Spacing (AIFS) values [20] may be used by nearby channels to avoid collisions, as suggested in [11]. All in all, further efforts are required in the design of more efficient techniques to face ACI, since this is serious problem for the simultaneous multi-channel operation in scenarios where nodes are in close proximity.

ACI is also a concern for future 5G mobile networks, since dynamic spectrum access will likely be employed to exploit spectrum holes in existing cellular networks. Therefore, new waveforms with high spectral efficiency and low Adjacent Channel Leakage Radio (ACLR) will be required in order to cause minimum impact in legacy systems, such as current 4G networks. Several experimental studies [21,22] are being conducted with the main goal of analyzing the possible coexistence of 5G and current LTE systems. Candidate waveforms such as Generalized Frequency Division Multiplexing (GFDM) that present lower ACLR and Peak-to-Average Power Ratio (PAPR) than traditional OFDM systems, are being tested and evaluated under these scenarios.

3. Effects of ACI in the received signal

This work addresses the problem of cross channel interference on the receiver nodes of a vehicular network, through the design of a digital two-stage FIR filter. The role of this filter is to attenuate the interfering signal on the adjacent channels as much as possible, while preserving the signal received in the desired frequency. As a first step in this design process, an experimental setup was devised to capture the raw samples at the receiver platform, when both the interferer node and the intended transmitter were sending messages. This way, an analysis can be performed on the characteristics of the received signal when ACI is present and thus, the filter design process can be optimized to strongly reject the spectral components of the unwanted signal.

3.1. Experimental setup

The setup used to fully characterize the ACI effect in the received digital baseband signal, took advantage of a research platform compliant with the IEEE 802.11p protocol [23]. The architecture of this flexible vehicular communication station, named IT2S platform, is presented in Fig. 2. There are two main components: a Single Board Computer where the higher layers of the protocol stack are implemented; and the IT2S Board, responsible for the MAC and physical layer's functionalities of IEEE 802.11p standard. In this experiment, the focus was on the analog to digital interface of the IT2S board, where the raw digital in-phase/quadrature (I/Q) samples were captured for analysis. The RF module down-converts the wireless signal to baseband, where it occupies half of the RF bandwidth, i.e. 5 MHz instead of 10 MHz, and then the AD/DA Converter, working at a sampling frequency of 40 MHz,

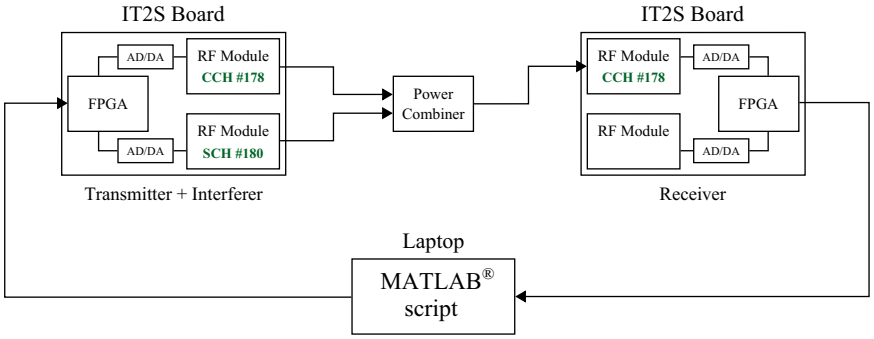

Fig. 3. Experimental setup used to analyze the effects of ACI in the received signal.

digitizes the signal before sending it to the FPGA.

The experiment was conducted in the scenario depicted in Fig. 3. Two IT2S platforms were employed, and since these are dual-radio devices as required by the ETSI ITS-G5 standards [4], a total of four radio units were available. Hence, one of the platforms was used as a transmitter and as an interferer simultaneously, with one radio tuned in the American control channel (CCH #178) and the other interfering in a adjacent service channel (SCH #180). The remaining IT2S platform was working as a receiver node with the radio where the digital I/Q samples were captured, operating in the CCH #178. All measurements were taken in a well-controlled environment, with all platforms directly connected through coaxial cables. A power combiner was used to couple the transmitted signal with the interfering one into the receiving radio. This way, the attenuation between the transmitter and the receiver was always constant and equal to the attenuation between the interferer and the receiver. The packet transmission in both radios was internally synchronized by the FPGA, forcing interference to actually happen. In the receiver node, the digital baseband samples coming from the AD/DA Converter were first stored and then retrieved from the FPGA directly to a computer, in order to be processed by a MATLAB® script. The Automatic Gain Control (AGC) mechanism was disabled in the receiving platform and a fixed gain value was used instead, in order to ensure that measurements were always taken under the same conditions.

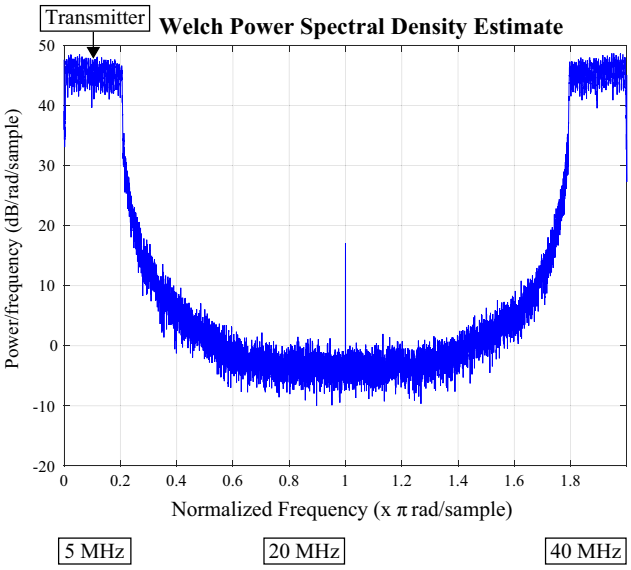

Fig. 4. Estimated power spectral density of the signal sent by the transmitter (tuned on CCH #178 and with a transmit power level of ≈ 7.5 dBm) at a sampling frequency of 40 MHz.

3.2. *Baseband ACI effect*

Firstly, only the radio tuned in the control channel #178 was transmitting, which allows the analysis of the received signal without interference. This way and after processing the digital raw I/Q samples recorded at the FPGA input, one can obtain a Power Spectral Density (PSD) estimate of the signal captured at the receiver node. Fig. 4 shows the baseband frequency domain representation of the signal transmitted on channel #178 with approximately 7.5 dBm of power. The graphics depicts the PSD estimate from 0 to 40 MHz – the ADC's sampling frequency. As it can be observed, the bandwidth of the signal is in fact 5 MHz, half of the 10 MHz occupied in the 5.9 GHz frequency band.

By keeping the same radio sending messages and adding the other one transmitting on SCH #180, one can observe the effect of ACI in the receiver node. This result is presented in Fig. 5, where it is visible the presence of the interfering baseband signal in a channel adjacent to the transmitter. The transmitting power was the same in both channels and it was equal to the one used in the experiment of Fig. 4, i.e. ≈ 7.5 dBm. It is clearly evident the difference in the spectral components from the case where there was no interferer. In baseband and from the perspective of the receiver tuned in channel #178, the interferer occupies a bandwidth of approximately 10 MHz, from 5 to 15 MHz. For these transmitting

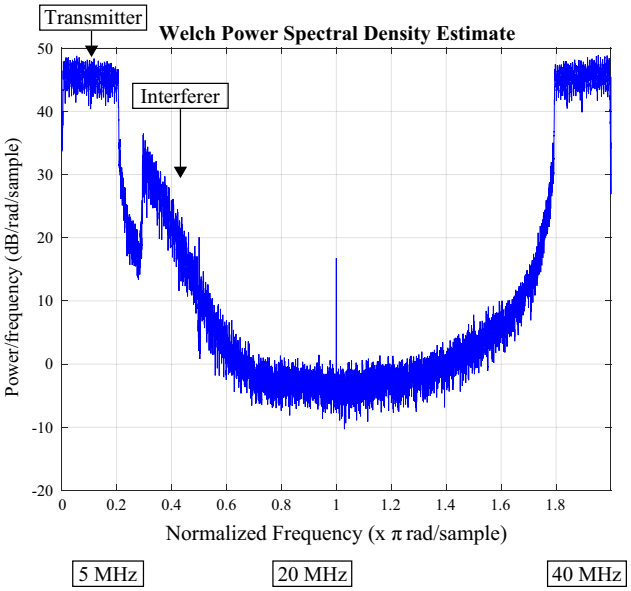

Fig. 5. Estimated power spectral density of the signals sent by the transmitter (CCH #178, ≈ 7.5 dBm) and the interferer (SCH #180, ≈ 7.5 dBm) at a sampling frequency of 40 MHz.

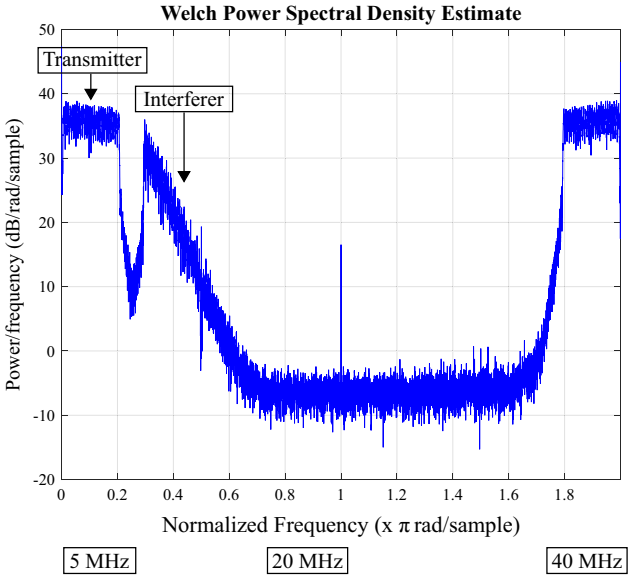

Fig. 6. Estimated power spectral density of the signals sent by the transmitter (CCH #178, ≈ -3 dBm) and the interferer (SCH #180, ≈ 27 dBm) at a sampling frequency of 40 MHz.

power levels, the peak of the unwanted signal in the frequency domain is approximately 15 dB below the signal received on the desired channel.

For the worst case scenario, i.e. when the transmitter is sending messages with the lowest power level available and the interferer is transmitting at full power, the PSD shown in Fig. 6 is obtained. In this situation, the peak of the interfering signal has almost the same value of the signal in the band of interest, being only 2 or 3 dB below. In conclusion, if no filtering operation is applied to the digital I/Q samples, the decoding process of the messages received in the scenarios presented in Figs. 5 and 6, will be seriously compromised. This problem derives from the fact that the unwanted signals in the nearby channels are not completely eliminated by the RF modules in the analog domain. In the IT2S platform, the RF module applies a low-pass filter with a cut-off frequency of 7.5 MHz, after down-converting the signal. Notice that in baseband the desired channel has a bandwidth of approximately 5 MHz and the immediate adjacent channel goes from ≈ 5 MHz to ≈ 15 MHz, thus the referred value of cut-off frequency is clearly insufficient. Under these circumstances, a more stringent filtering operation should be performed in the digital domain, using a lower cut-off frequency and a shorter transition band.

4. Digital interpolated FIR filter

Based on the previous results, it can be concluded that an interfering signal in an adjacent channel could severely affect the proper reception of messages sent by a transmitter node tuned in the channel of interest. The level of the signal generated by the interferer that appears at the FPGA input could be approximately equal to (Fig. 6) or even greater than the desired signal (a situation that would occur if an attenuator was added between the transmitter and the power combiner in the setup above, making the path loss of the interferer lower than the one of the transmitter). This interference has to be filtered in order to increase the probability of correctly decoding the received messages and to avoid the false blocking transmission effect described in Section 2. In this paper, the design and evaluation of a two-stage FIR low-pass filter are presented, with the main goal of reducing the interference due to the adjacent channels. The first stage is constituted by an

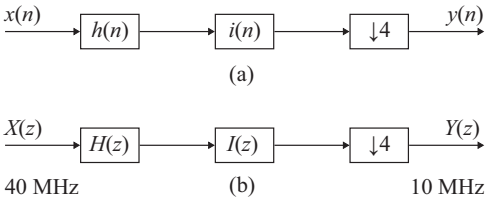

Fig. 7. Block diagram of the two-stage low-pass filter, both in (a) time and (b) frequency domains.

interpolated FIR filter, which is more efficient than a simple FIR filter, since it can achieve steeper slopes with the same filter order. However, it needs another low-pass filter to eliminate the undesired passbands resulting from interpolation. The design of this second low-pass filter is not so stringent, i.e. requires a lower filter order, and it could be implemented with a polyphase decomposed architecture, consuming few FPGA resources and taking advantage of the decimation factor of 4 that could be applied to the I/Q samples. This decimation can take place since there was an oversampling factor of 4 in the AD/DA Converter. In other words, the signal with a bandwidth of 5 MHz was sampled at 40 MHz, four times more than the required by the Nyquist theorem.

The block diagram, both in time and frequency domains, of the two-stage low-pass filter is presented in Fig. 7. The signal $x(n)$ or $X(z)$ represents the digital raw I/Q samples at the FPGA input. Then, $h(n)$ or $H(z)$ corresponds to the first stage of the filtering process – the Interpolated FIR (IFIR) filter, responsible for implementing the narrow transition band immediately after the spectrum components of the signal in the desired channel. The second stage is constituted by the polyphase decomposed filter $i(n)$ or $I(z)$, taking advantage of the decimation factor of 4, whose goal is to eliminate the frequency replicas not attenuated by the interpolated FIR filter. Finally, $y(n)$ or $Y(z)$ represents the filtered signal that will feed the digital receiver chain at a sampling rate of 10 Msps. The detailed block diagram of this two-stage low-pass filter is depicted in Fig. 8. This scheme could be easily implemented in digital hardware (FPGA) using simple processing blocks, like adders, multipliers and registers for the time delays.

The coefficients for the design of both filters were obtained in MATLAB® with the aid of Filter Design and Analysis Tool (FDAtool). For the IFIR filter, these coefficients were first computed for an equiripple FIR filter without interpolation. However, since an interpolation factor of 3 was then applied, the specified transition band was three times larger than the desired filter. After that, the design of the final IFIR filter can be concluded, by adding two null coefficients between two consecutive coefficients previously obtained in FDAtool. These zero value coefficients are naturally omitted in the top part of Fig. 8 but are implicit in the delays of 3 units (z^{-3}). The complete specifications used in the fdatool for this filter with minimum order are presented in Table 1. A passband frequency of 4.14 MHz was specified instead of 5 MHz, since the standard imposes a small band guard value of ≈ 800 kHz in each side of vehicular channels, so the actual RF bandwidth is not exactly 10 MHz but approximately $10 - (2*0.8)$ MHz. For the given input parameters, a minimum filter order of $N=29$ was obtained. The frequency response of the IFIR filter is presented in Fig. 9. The additional passbands resulting from the interpolation process are easily noticed, occupying a baseband spectrum between ≈ 0.45 and 0.9π rad/sample in normalized units, which corresponds to the frequency range between ≈ 9 and 18 MHz.

Following the design phase, the IFIR filter was applied to the original signal from Fig. 6, using MATLAB® code that simulates an efficient implementation in hardware, where the multipliers corresponding to the null coefficients were eliminated, just like in Fig. 8. The PSD of the signal obtained at the output of the IFIR filter is shown in Fig. 10. One can observe the strong attenuation of

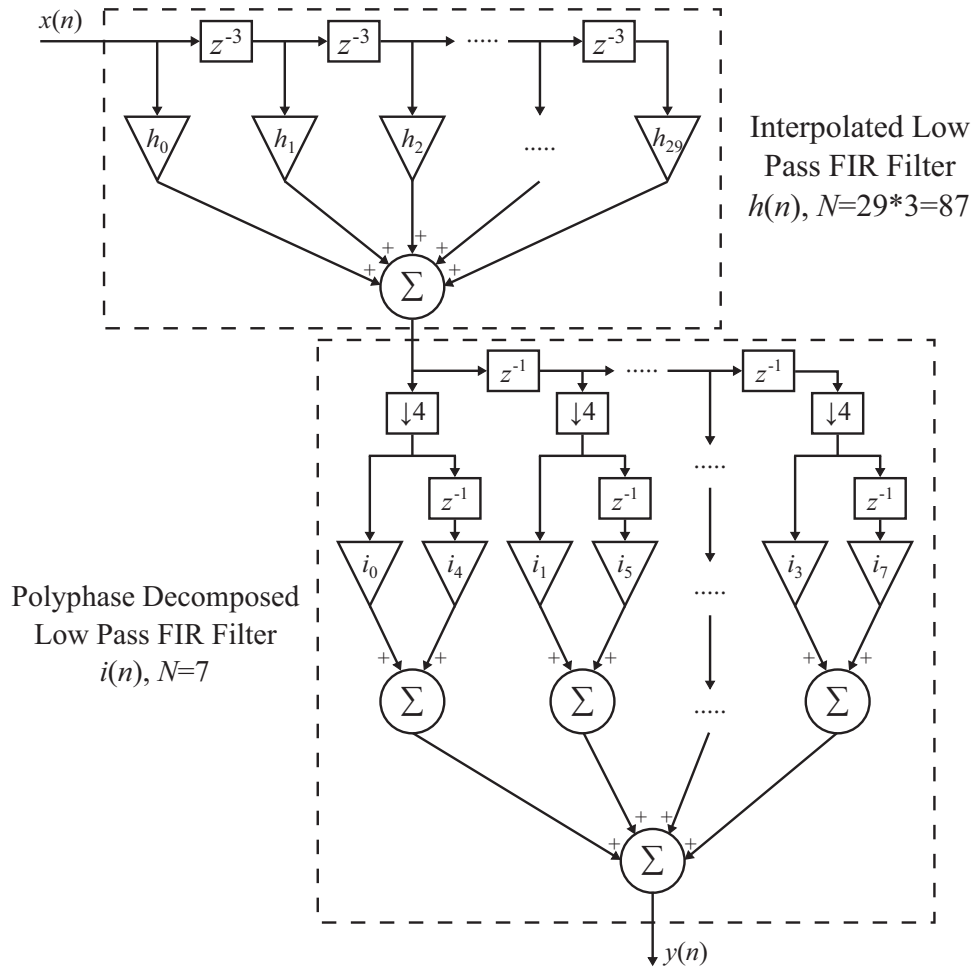

Fig. 8. Detailed block diagram of both the interpolated low-pass FIR filter (top) and the polyphase decomposed low-pass FIR filter (bottom).

Tab. 1
Interpolated FIR filter parameters in FDA tool.

Response type	Lowpass
Filter order (minimum order)	29
Design method	FIR equiripple
Sampling frequency (Fs)	40 MHz
Absolute passband	3*4.14 MHz
Frequency (Fpass)	=12.42 MHz
Normalized passband	3*0.207π rad
Frequency (wpass)	=0.621π rad
Absolute stopband	3*4.88 MHz
Frequency (Fstop)	=14.64 MHz
Normalized stopband	3*0.244π rad
Frequency (wstop)	=0.732π rad
Passband attenuation (Apass)	0.5 dB
Stopband attenuation (Astop)	40 dB

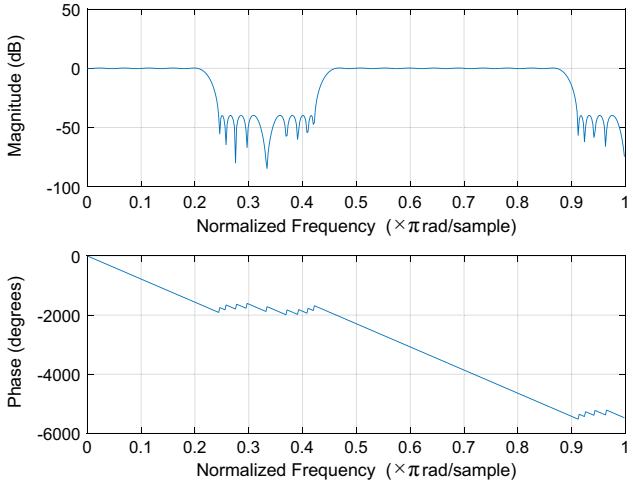

Fig. 9. Frequency response of the $H(z)$ low-pass IFIR filter.

nearly 40 dB in the peak of the original interfering signal (the gray one). However, there are replicated passbands that have to be eliminated by the second low-pass filter $I(z)$. This filter was also created in fdatool with the parameters displayed in Table 2. In this case, a filter order of $N=7$ was specified and a stopband frequency of 8.42 MHz was required in order to remove the replicas starting at ≈ 9 MHz. The frequency response of this second filter is presented in Fig. 11. As it can be seen, the transition band is more relaxed and the attenuation in the stopband is lower than the case of the IFIR filter, because a lower filter order was utilized and the frequency requirements were not so stringent. Nevertheless, these filter characteristics are sufficient to mitigate the impact of the replicated passbands in the filtered signal, represented by the black PSD in Fig. 12. The result presented in this figure is obtained before the decimation block in Fig. 6, which means that in this case the polyphase decomposition property was not applied yet. The PSD of the output signal shows that the peak value of the interferer (≈ -5 dB/rad/sample at $\approx 0.5\pi$ rad) was attenuated by 40 dB when compared to the original signal (≈ 35 dB/rad/sample at $\approx 0.3\pi$ rad). This constitutes a strong reduction in the amount

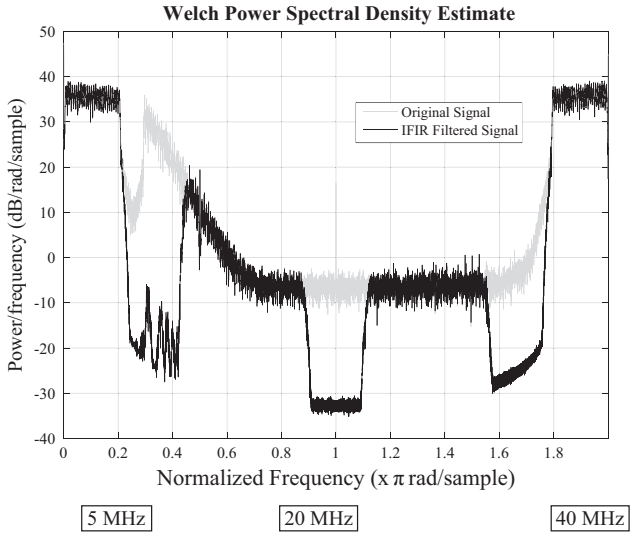

Fig. 10. Estimated power spectral density comparison between the original signal from Fig. 6 (in gray) and the signal obtained after the $H(z)$ filter (in black) at a sampling frequency of 40 MHz.

Tab. 2
Polyphase decomposed FIR filter parameters in fdatool.

Response type	Lowpass
Filter order (specify order)	7
Design method	FIR equiripple
Sampling frequency (Fs)	40 MHz
Absolute passband frequency (Fpass)	4.14 MHz
Normalized passband frequency (wpass)	0.207π rad
Absolute stopband frequency (Fstop)	8.42 MHz
Normalized stopband frequency (wstop)	0.421π rad
Passband weight value (Wpass)	10
Stopband weight value (Wstop)	1

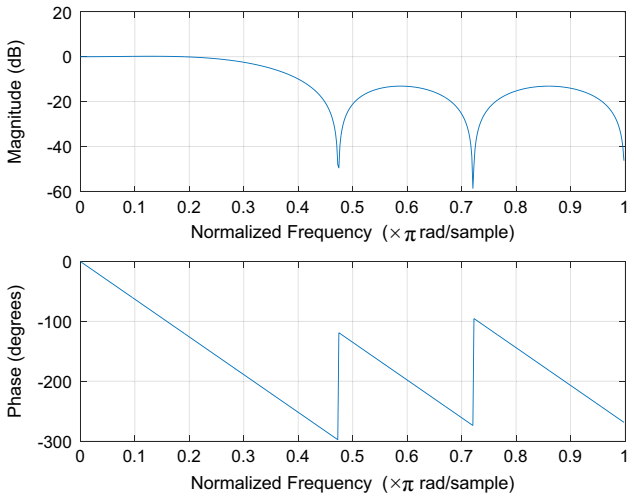

Fig. 11. Frequency response of the $I(z)$ low-pass FIR filter.

of interference present in the received signal and increases the probability of successfully decoding the packets by the receiver node.

By taking advantage of the decimation factor of 4 (Fig. 7), the implementation of the $I(z)$ filter can be made more efficient, being the filtering operation performed at a lower data rate (10 Msps instead of 40 Msps). In this way, a polyphase decomposition with 4 phases can be employed, as depicted in Fig. 13. Thus, the polyphase decomposed $I(z)$ filter takes the shape of the block diagram

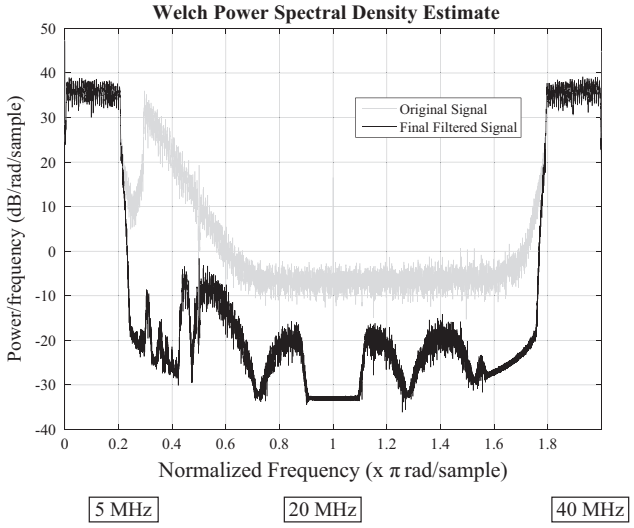

Fig. 12. Estimated power spectral density comparison between the original signal from Fig. 6 (in gray) and the signal obtained after the $I(z)$ filter (in black) at a sampling frequency of 40 MHz.

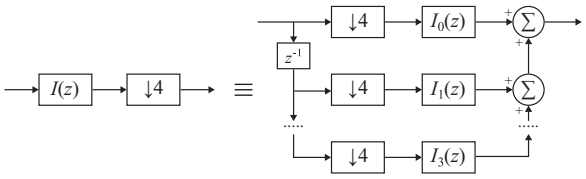

Fig. 13. Polyphase decomposed filter with a decimation factor of 4.

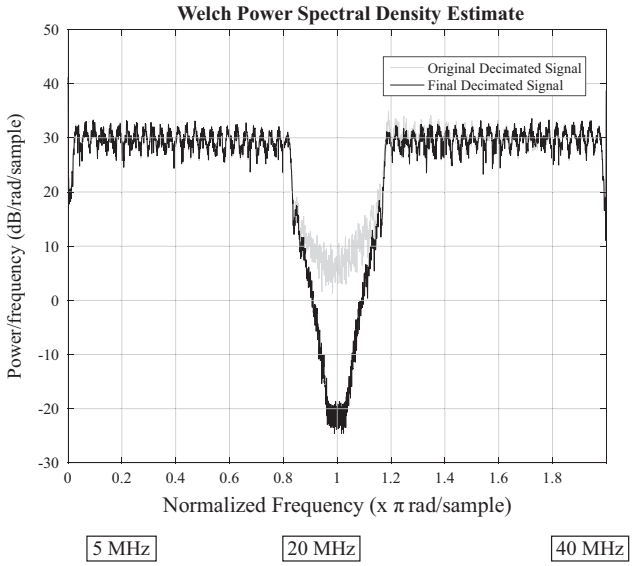

Fig. 14. Estimated power spectral density comparison between the original signal solely decimated (in gray) and the final signal obtained after the designed two-stage low-pass filter (in black) at a sampling frequency of 10 MHz.

presented in the bottom part of Fig. 8.

Finally, a comparison can be performed between the original situation, where the captured data was solely decimated before being processed by the digital receiver chain, and the case where the two-stage low-pass filter proposed in this paper was employed. The spectrum analysis of both resulting signals is shown in Fig. 14. The PSDs presented here correspond to the samples that would be supplied as an input to the receiver chain operating at a sampling rate of 10 Msps, thus already include the effect of the decimation by a factor of 4. As it can be observed, the transition

band of the filtered signal is much sharper and an attenuation of almost 30 dB has been achieved at half of the sampling frequency.

In terms of the delay introduced in the receiver chain, its value is given by adding the delay imposed by both filters. Regarding the IFIR filter, the order of the filter built in the fdatool has to be multiplied by 3, to take into account the effect of interpolation and the zero-value coefficients added at the end. Consequently, the IFIR filter order is equal to $N=29*3=87$ and therefore, the group delay is equivalent to $((87+1)/2)=44$ clock cycles at 40 MHz, which corresponds to an absolute delay of 1.1 μs. In what concerns to the polyphase decomposed FIR filter, giving that its order is $N=7$, a group delay of $(7+1)/2=4$ clock cycles at 40 MHz is introduced, corresponding to an absolute delay of 0.1 μs. As a result, a total delay of 1.2 μs is added to the receiver chain by the cascade of the two low-pass filters. This value is perfectly acceptable for the system's operation, given the 12.8 μs available to perform frame detection and automatic gain control [2].

5. Conclusions and future work

In this paper, a two-stage low-pass FIR filter has been proposed with the main goal of mitigating the effects of adjacent channel interference in vehicular communication systems. First, an interpolated FIR filter with a narrow transition band was designed to strongly attenuate the spectral components of the interfering signal close to the desired channel. And then, a polyphase decomposed FIR filter was employed to eliminate the passband replicas of the IFIR filter. The design followed a multi-rate approach, taking advantage of the decimation block in the interface between the analog and the digital domains of the receiver chain.

The behavior of this two-stage filter was simulated and tested in MATLAB® and the results have shown that the proposed solution significantly reduces the impact of the adjacent channel transmissions in the signal of interest. Furthermore, the cascade of the two filters can be efficiently implemented in an FPGA, consuming simple digital hardware blocks. In addition, only a small delay is introduced in the decoding process of the receiving platform.

As future work, the designed filter will be implemented in an FPGA and integrated in the operation of the IT2S platform. This way, it will be possible to evaluate the performance of the proposed solution in a real-world scenario. Metrics such as packet error rates, could be analyzed under the presence of an interfering node, and the statistics could be compared with the present situation, where no filtering operation is involved.

Acknowledgments

This work is funded by National Funds through FCT - Fundação para a Ciência e a Tecnologia under the PhD scholarship Ref. SFRH/BD/52591/2014 and the project PEst-OE/EEI/LA0008/2013, by the European Union's Seventh Framework Programme (FP7) under grant agreement no. 3176711 and by BRISA, under research contract with Instituto de Telecomunicações - Aveiro.

References

[1] C. Campolo, A. Molinaro, Multichannel communications in vehicular ad hoc networks: a survey, IEEE Commun. Mag. 51 (5) (2013) 158–169, http://dx.doi.org/10.1109/MCOM.2013.6515061.

[2] IEEE Standard for Information Technology–telecommunications and information exchange between systems local and metropolitan area networks–specific requirements, Part 11: Wireless LAN Medium Access Control (MAC) and Physical Layer (PHY) Specifications, IEEE Std 802.11-2012 (Revision of IEEE Std 802.11-2007), 2012, pp. 1–2793.

[3] J. Kenney, Dedicated short-range communications (DSRC) standards in the United States, Proc. IEEE 99 (7) (2011) 1162–1182, http://dx.doi.org/10.1109/JPROC.2011.2132790.

[4] ETSI, Final draft ETSI ES 202 663 V1.1.0 (2009–11), ETSI standard, intelligent transport systems (ITS); European profile standard for the physical and medium access control layer of intelligent transport systems operating in the 5 GHz frequency band, November 2011.

[5] ECC Report 101, Compatibility Studies in the Band 5855–5925 MHz Between Intelligent Transport Systems (ITS) and Other Systems, Bern, February 2007.

[6] ETSI TR 102 654 (V1.1.1), Electromagnetic Compatibility and Radio Spectrum Matters (ERM); Road Transport and Traffic Telematics (RTTT); Co-location and Co-existence Considerations Regarding Dedicated Short Range Communication (DSRC) Transmission Equipment and Intelligent Transport Systems (ITS) Operating in the 5 GHz Frequency Range and Other Potential Sources of Interference, January 2009.

[7] ETSI TS 102 792 (V1.2.1), Intelligent Transport Systems (ITS); Mitigation Techniques to Avoid Interference Between European CEN Dedicated Short Range Communication (CEN DSRC) Equipment and Intelligent Transport Systems (ITS) Operating in the 5 GHz Frequency Range, June 2015.

[8] ETSI EN 302 571 (V1.2.0), Intelligent Transport Systems (ITS); Radio Communications Equipment Operating in the 5855 MHz to 5925 MHz Frequency Band; Harmonized EN Covering the Essential Requirements of Article 3.2 of the R&TTE Directive, May 2013.

[9] ETSI TR 102 960 (V1.1.1), Intelligent Transport Systems (ITS); Mitigation Techniques to Avoid Interference Between European CEN Dedicated Short Range Communication (RTTT DSRC) Equipment and Intelligent Transport Systems (ITS) Operating in the 5 GHz Frequency Range; Evaluation of Mitigation Methods and Techniques, November 2012.

[10] K. chan Lan, C.-M. Chou, D.-J. Jin, The effect of 802.11a on DSRC for ETC communication in: 2012 IEEE Wireless Communications and Networking Conference (WCNC), 2012, pp. 2483–2487. http://dx.doi.org/10.1109/WCNC.2012.6214215.

[11] C. Campolo, A. Molinaro, A. Vinel, Understanding adjacent channel interference in multi-channel VANETs, in: 2014 IEEE Vehicular Networking Conference (VNC), 2014, pp. 101–104. http://dx.doi.org/10.1109/VNC.2014.7013316.

[12] T. Pham, I. McLoughlin, S. Fahmy, Shaping spectral leakage for IEEE 802.11p vehicular communications, in: 2014 IEEE 79th Vehicular Technology Conference (VTC Spring), 2014, pp. 1–5. http://dx.doi.org/10.1109/VTCSpring.2014.7023089.

[13] V. Rai, F. Jai, J. Kenney, K. Laberteaux, Cross-Channel Interference Test Results: A Report from the VSC-A Project, IEEE 802.11 11-07-2133-00-000p, July 2007.

[14] R. Lasowski, F. Gschwandtner, C. Scheuermann, M. Duchon, A multi channel synchronization approach in dual radio vehicular ad-hoc networks, in: 2011 IEEE 73rd Vehicular Technology Conference (VTC Spring), 2011, pp. 1–5. http://dx.doi.org/10.1109/VETECS.2011.5956640.

[15] C. Campolo, H. Cozzetti, A. Molinaro, R. Scopigno, Overhauling ns-2 PHY/MAC simulations for IEEE 802.11p/WAVE vehicular networks, in: 2012 IEEE International Conference on Communications (ICC), 2012, pp. 7167–7171. http://dx.doi.org/10.1109/ICC.2012.6364771.

[16] W. Cho, G. Lee, B. Park, PER measurement of vehicular communication systems with adjacent channel interferences, in: G. Lee, D. Howard, D. Ślęzak, Y. Hong (Eds.), Convergence and Hybrid Information Technology, Communications in Computer and Information Science, vol. 310, Springer, Berlin, Heidelberg, 2012, pp. 46–52. http://dx.doi.org/10.1007/978-3-642-32692-9_7.

[17] N. Vivek, S. Srikanth, P. Saurabh, T. Vamsi, K. Raju, On field performance analysis of IEEE 802.11p and WAVE protocol stack for V2V amp; V2I communication, in: 2014 International Conference on Information Communication and Embedded Systems (ICICES), 2014, pp. 1–6. http://dx.doi.org/10.1109/ICICES.2014.7033960.

[18] Y. Bi, K.-H. Liu, L. Cai, X. Shen, H. Zhao, A multi-channel token ring protocol for QoS provisioning in inter-vehicle communications, IEEE Trans. Wireless Commun. 8 (11) (2009) 5621–5631, http://dx.doi.org/10.1109/TWC.2009.081651.

[19] C. Campolo, A. Molinaro, Improving multi-channel operations in VANETs by leveraging stopped vehicles, in: 2013 IEEE 24th International Symposium on Personal Indoor and Mobile Radio Communications (PIMRC), 2013, pp. 2229–2233. http://dx.doi.org/10.1109/PIMRC.2013.6666514.

[20] C. Campolo, A. Molinaro, A. Vinel, Y. Zhang, Modeling prioritized broadcasting in multichannel vehicular networks, IEEE Trans. Veh. Technol. 61 (2) (2012) 687–701, http://dx.doi.org/10.1109/TVT.2011.2181440.

[21] M. Danneberg, R. Datta, G. Fettweis, Experimental testbed for dynamic spectrum access and sensing of 5G GFDM waveforms, in: 2014 IEEE 80th Vehicular Technology Conference (VTC Fall), 2014, pp. 1–5. http://dx.doi.org/10.1109/VTCFall.2014.6965979.

[22] F. Kaltenberger, R. Knopp, M. Danneberg, A. Festag, Experimental analysis and simulative validation of dynamic spectrum access for coexistence of 4g and future 5g systems, in: 2015 European Conference on Networks and Communications (EuCNC), 2015, pp. 497–501. http://dx.doi.org/10.1109/EuCNC.2015.7194125.

[23] J. Almeida, J. Ferreira, A. Oliveira, Development of an ITS-G5 station, from the physical to the MAC layer, in: Intelligent Transport Systems: from Good Practice to Standards, CRC Press, Vancouver, Canada, 2016.